

Real-time PET analysis of metastatic tumor cell trafficking in vivo and its relation to adhesion properties

Chieko Koike ^a, Naoto Oku ^{a,*}, Manabu Watanabe ^a, Hideo Tsukada ^{b,c}, Takeharu Kakiuchi ^b,
Tatsuro Irimura ^d, Shoji Okada ^a

^a Department of Radiobiochemistry, School of Pharmaceutical Sciences, University of Shizuoka, 52-1 Yada, Shizuoka, 422 Japan

^b Center Research Laboratory, Hamamatsu Photonics, Hamakita, Shizuoka, Japan

^c Subfemtomole Biorecognition Project, Research Development Corporation of Japan, Hamakita, Shizuoka, Japan

^d Division of Chemical Toxicology and Immunochemistry, Faculty of Pharmaceutical Sciences, The University of Tokyo, Bunkyo-ku, Tokyo, Japan

Received 30 November 1994; accepted 13 April 1995

Abstract

Although a number of studies have indicated that highly metastatic cells tend to adhere more to target endothelium in vitro than low or non-metastatic cells, direct evidence about the correlation between cellular adhesiveness and organ disposition of the cells has not been obtained. Using positron emission tomography (PET), we have developed a novel technique that enables the non-invasive detection of the real-time tumor cell trafficking. The present study shows the correlation between trafficking of murine large cell lymphoma RAW117 and the adhesion properties of the cells in vitro. Cells accumulated in the liver time-dependently, and accumulation of RAW117-H10, liver metastatic subline cells, was more intense than that of RAW117-P, the parental cells, indicating that the metastatic potential is correlated with the in vivo accumulation of the cells in the target tissue. To examine whether the adhesion properties of the cell membrane determine the cell trafficking, we performed PET analysis after altering the adhesion properties on the cell membrane by means of cellular protein kinase C modulation, since the modulation of this enzyme is known to alter the surface adhesion molecules, i.e., those of the integrin superfamily. The treatment of RAW117-P with 12-*O*-tetradecanoylphorbol 13-acetate, which caused augmentation of adhesion to hepatic sinusoidal microvessel endothelial cells (HSE) in vitro, enhanced the hepatic accumulation of the cells in vivo. On the contrary, treatment of RAW117-H10 with the protein kinase C inhibitor H-7, 1-(5-isoquinolinesulfonyl)-2-methylpiperazine dihydrochloride, which reduced the adhesion activity of the cells to HSE, suppressed their accumulation in the liver, although the suppression was observed only during the first 30 min after administration of the cells. These data suggest that the adhesion properties of metastatic lymphoma cells are critical for the accumulation of these cells in the target tissue.

Keywords: Positron emission tomography (PET); Tumor metastasis; Protein kinase C; Cell trafficking; RAW117 large cell lymphoma; Lymphoma cell

1. Introduction

Metastasis proceeds in multiple steps: blood-borne metastasis is thought to occur via platelet-aggregation, adhesion of the metastatic cells to the target endothelial cells, and invasion into the extracellular matrix. Escape from the immune defense system is also important. We recently developed a non-invasive technique using positron emission tomography (PET) to determine the real-time trafficking of tumor cells in vivo, and observed that cells of a highly metastatic subline showed intense accumulation in the target organ, in a lung metastatic model, rat

13762NF mammary adenocarcinoma [1]. This technique is useful to evaluate the interaction of characteristic metastatic tumor cells with various organs in a living animal without affecting in vivo circumstances such as blood flow.

The lung accumulation of the cells, however, is difficult to analyze, however, since the lung is a first-pass tissue when the cells are injected intravenously. Therefore, we examined cell trafficking using a hepatic metastatic model, namely, the parental murine RAW117 large cell lymphoma of low metastatic potential (RAW117-P) and its subline having high metastatic potential for the liver (RAW117-H10), selected in vivo by Brunson and Nicolson [2], in the present study to examine the relationship between organ-specific metastasis and interaction of the cells with the target organ at the early stage of experimental metastasis.

* Corresponding author. Fax: +81 54 2645705.

Furthermore, to examine whether the cellular surface properties of the tumor cells determine the interaction of the cells with the target organ, trafficking of the same kind of cells whose surface properties were altered by the modulation of intracellular protein kinase C (PKC) was monitored, since the modulation of PKC is known to affect both metastatic potential and surface molecules, i.e., those of the integrin superfamily.

2. Materials and methods

2.1. Cell preparation for PET analysis

RAW117 parental line (RAW117-P) and a variant sub-line (RAW117-H10) sequentially selected ten times *in vivo* for liver colonization were kindly donated by Dr.

Nicolson of the University of Texas. These cells were cultured in high-glucose DMEM supplemented with 5% fetal calf serum (JRH Biosciences, Lenexa, KS) under a humidified atmosphere of 5% CO₂ in air. The cells were labeled with [2-¹⁸F]FDG by a modified method described previously [1]. In brief, the cells were washed with glucose-free medium and incubated with [2-¹⁸F]FDG for 15 min at 37°C, since the incorporation of FDG reached a plateau at about 15 min as determined by use of [¹⁴C]FDG (data not shown). After the cells had been washed to remove the free [2-¹⁸F]FDG by centrifugation at 600 × *g* for 10 min, a single cell suspension was obtained.

2.2. PET analysis of cell trafficking

PET studies were performed with an animal PET camera (Hamamatsu Photonics, Hamamatsu, Japan, HSR-2000)

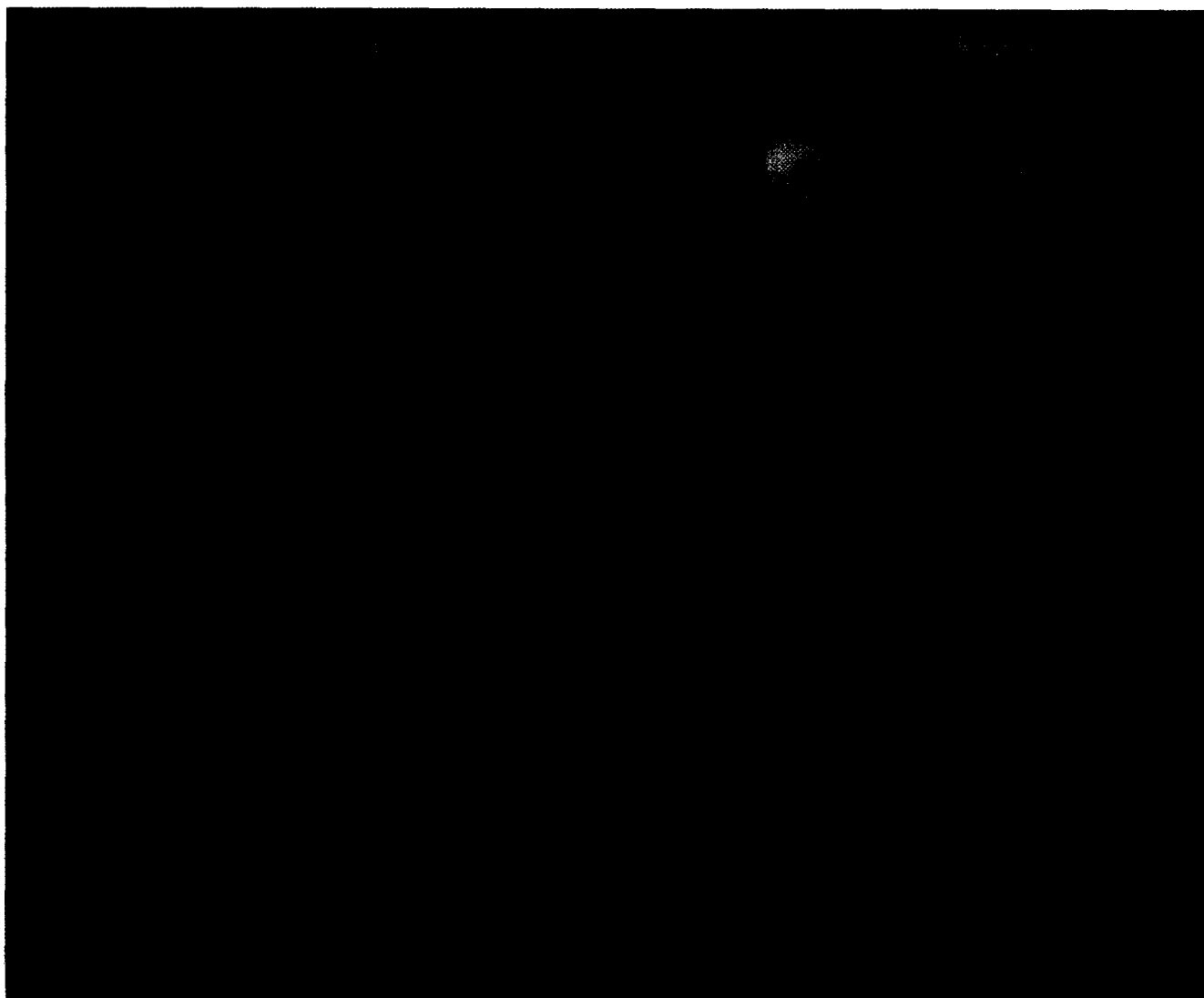


Fig. 1. PET images of metastatic lymphoma cell trafficking *in vivo*. Biodistribution during 30 min after administration of [2-¹⁸F]FDG-labeled RAW117-P and RAW117-H10 was imaged by PET. All images are in a coronal plane with a slice size of 3 mm. For reference to PET images, X-ray CT images of lungs, heart, liver, and kidneys of a mouse of similar age are presented in the top panel. Gradation was corrected to be comparable between liver and kidney. The image intensities of lungs and heart are 8-fold higher than those of liver and kidney.

having an effective slice aperture of 3.25 mm and resolution of 2.7 mm. RAW117-P or -H10 cells labeled with [^{18}F]FDG ($1 \cdot 10^6$ cells in 0.2 ml high glucose DMEM, 555 kBq–925 kBq) were injected via a tail vein into 10-week-old female Balb/c mice (Japan SLC, Hamamatsu, Japan) anesthetized with sodium pentobarbital. The emission scan of PET was started immediately after injection and performed for 90 min. Before injection of the cells, transmission scans were obtained by use of an 18.5 MBq $^{68}\text{Ge}/^{68}\text{Ga}$ ring source for attenuation correction. The radioactivity in the form of coincidence gamma photons was measured and converted to Bq/cm³ of tissue volume by calibration after correction for decay and attenuation. A time-activity curve was obtained from the mean pixel radioactivity in the region of interest (ROI) of the composed PET images where ROIs that covered the liver image were chosen. The injected dose in each experiment was normalized as 740 kBq throughout the whole study. Each PET experiment presented in this paper was repeated at least twice, and similar results were obtained for those repeated experiments; although each figure represents a typical result obtained from a single experiment.

After every PET measurement, animals were killed for removal of organs and counting of the radioactivity in these organs with an auto gamma counter to confirm the accumulation of cells in each organ. ROI values of each organ correlated with the result of the direct counting of the radioactivities in each organ. The viability of remaining cells after administration of the cells was determined at 2 h after initiation of PET scan by Trypan blue dye exclusion and the viability of cells was more than 90% throughout the whole experiment.

2.3. X-ray CT analysis

Ten-week-old female Balb/c mice were anesthetized with sodium pentobarbital and X-ray CT images were obtained. Slice distances were 3.2 mm.

2.4. Cell adhesion assay

Hepatic sinusoidal microvessel endothelial cells (HSE) of less than 15 passages, kindly provided by Dr. Nicolson of the University of Texas, were seeded in 24-well culture dishes ($2 \cdot 10^5$ cells/well) in DME/Ham's F12 medium containing bovine endothelial mitogen (Biomedical Technologies, Stoughton, MA). RAW117 cells were fluorescence-labeled by incubation with 30 μM 3'-O-acetyl-2',7'-bis(carboxyethyl)-4- or 5-carboxyfluorescein, diacetoxymethyl ester (BCECF-AM, Dojindo Laboratories, Kumamoto, Japan) for 30 min at 37°C [3]. After the labeled cells had been washed with PBS, $5 \cdot 10^4$ of them were added into each well of a 24-well culture dish preseeded with HSE. After a 30-min or 1-h incubation, the non-adherent cells were removed, and adherent cells were lysed with 1% Triton X-100. The percentage of adherent cells was determined fluorometrically.

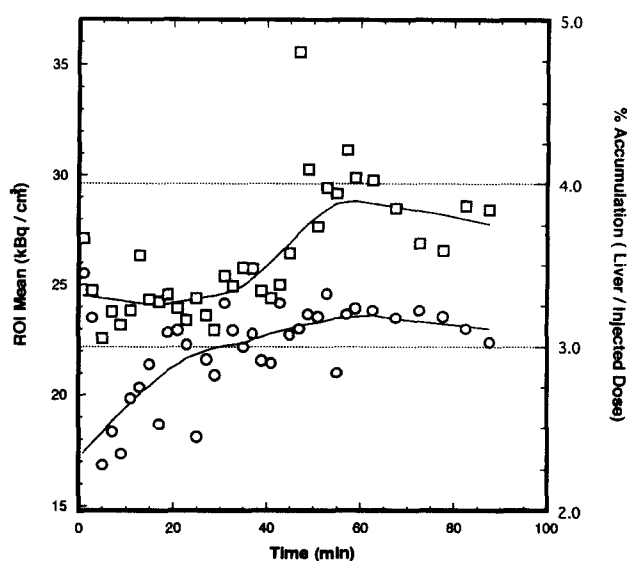


Fig. 2. Time-activity curves of ^{18}F accumulation in the liver after injection of [^{18}F]FDG-labeled RAW117 cells. Time-activity curves of ^{18}F in the liver after injection of [^{18}F]FDG-labeled RAW117-P (○) and RAW117-H10 (□) were obtained as described in Materials and methods.

2.5. Modulation of intracellular protein kinase C activity

For activation of PKC in RAW117-P, the cells were treated with 0.162 μM 12-O-tetradecanoylphorbol 13-acetate (TPA, Sigma, St. Louis, MO) for 1 h at 37°C. After removal of TPA, the cells were labeled with [^{18}F]FDG and applied for PET scanning, or cells were labeled with BCECF-AM and applied for adhesion assays with HSE. For the inactivation of PKC in RAW117-H10, cells were treated with 200 μM 1-(5-isoquinolinesulfonyl)-2-methylpiperazine dihydrochloride (H-7, Biomol Research, Ply-

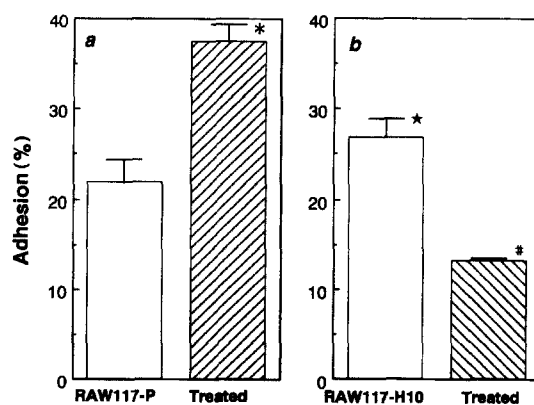


Fig. 3. Effect of protein kinase C modulators on RAW117 cell adhesion to HSE. (a) RAW117-P cells were treated with 0.162 μM TPA for 1 h, and the amount of fluorescence of cells adhering to HSE was determined as described in Materials and methods. (b) RAW117-H10 cells were treated with 200 μM H-7 for 2 h, and the amount of HSE-associated fluorescence was determined. Significant differences are shown in the figure: *, $P < 0.001$ when compared with RAW117-P; ★, $P < 0.05$ when compared with RAW117-P; #, $P < 0.01$ when compared with RAW117-H10.

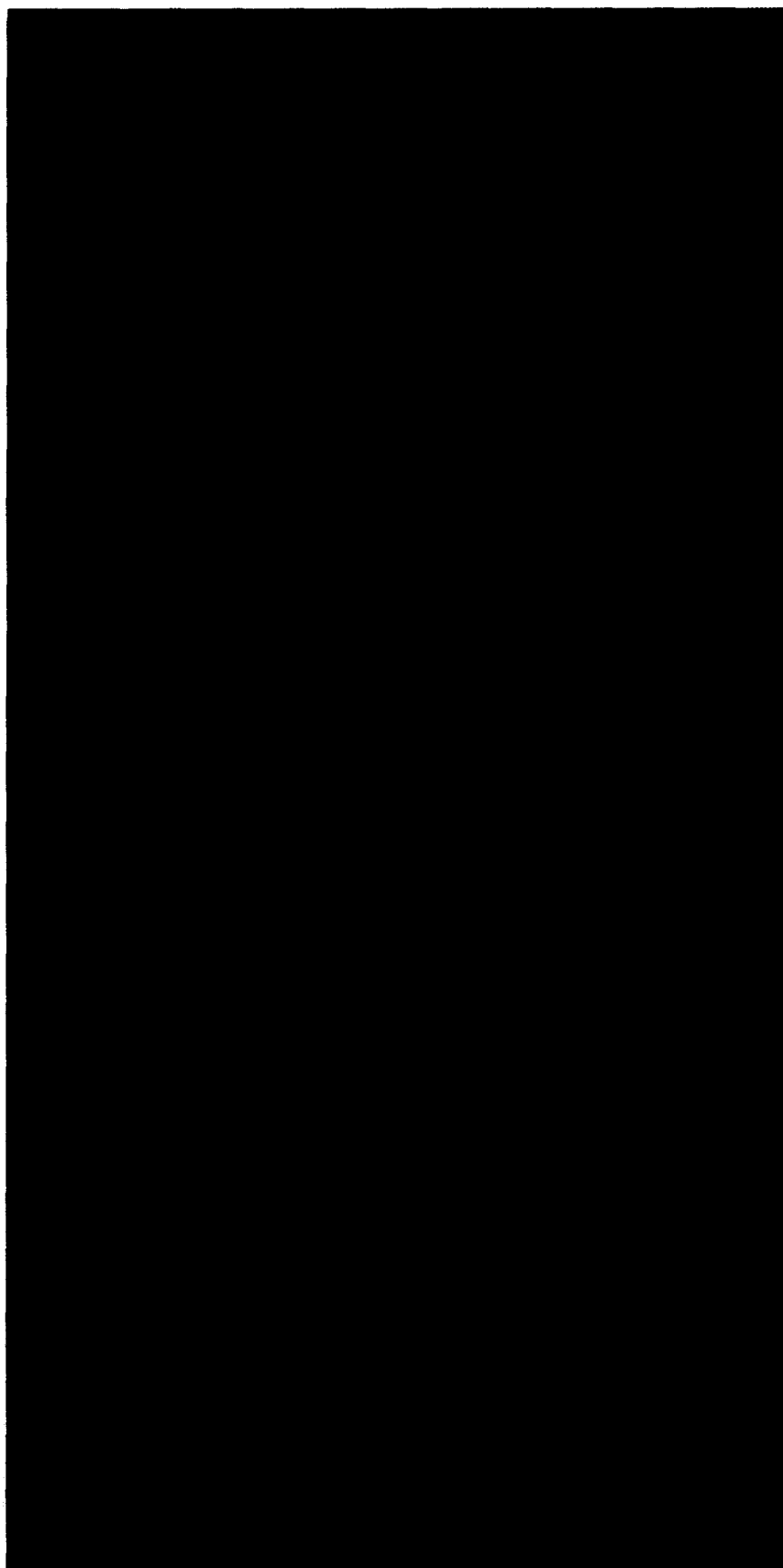


Fig. 4. Effect of TPA on RAW117-P cell accumulation in the liver. Liver accumulation of [2-¹⁸F]FDG-labeled RAW117-P treated or not with TPA was determined by PET as described in Materials and methods. Status of the accumulation of the cells during the first 30 min after injection of the cells; during the next 30 min, and during 60-to-90 min period post injection is shown.

mouth Meeting, PA) for 2 h at 37°C. Then, PET analysis and adhesion assay were performed similarly as for TPA-treated RAW117 cells.

3. Results

3.1. Metastatic tumor cell trafficking determined by PET

For PET analysis of these cells, the cells were labeled with [2-¹⁸F]FDG in vitro and intravenously injected into the bloodstream of mice. Fig. 1 shows PET images during the first 30 min after injection of the cells. X-ray CT images are also shown in the top panel of the figure. RAW117-H10 cells accumulated in the liver at a higher rate than RAW117-P cells. Both types of cells accumulated in the lungs, although the number of retained cells decreased rapidly as compared with the retention in the liver (data not shown). Fig. 2 indicates the time-activity curves of RAW117-P and RAW117-H10 accumulation in the liver. The accumulation of RAW117-H10 was more intense than that of RAW117-P during the PET measurement, indicating strong interaction of liver metastatic RAW117-H10 cells with liver endothelium in vivo and confirming the metastasis of the cells to the liver.

3.2. Effect of protein kinase C modulators on RAW117 cell trafficking

Recently, PKC was reported to regulate tumor cell adhesion to endothelium and extracellular matrix [4–11]. Furthermore, integrins were reported to be the substrates for both PKC [12,13] and tyrosine kinases [14]. Therefore, the trafficking of tumor cells might be altered when PKC activity is modulated. So we examined the adhesion of RAW117 cells to HSE in vitro under conditions where PKC activity was changed. As shown in Fig. 3, in agreement with previous observations [15], the rate of adhesion of highly metastatic RAW117-H10 cells to HSE was higher than that of low metastatic RAW117-P cells. Furthermore, adhesion of RAW117-P to HSE was increased more than 70% by treatment with TPA. Adhesion of RAW117-H10 to HSE was suppressed to nearly 50% after treatment with H-7. These observations suggest that PKC activity is related to the adhesion of RAW117 cells to HSE.

Subsequently, we investigated in vivo the trafficking of RAW117 cells after modulating PKC activities. Fig. 4 shows the PET images of hepatic accumulation of RAW117-P cells with or without TPA treatment. In this experiment, the treatment did not affect FDG uptake or viability at least until the termination of the PET scanning. Corresponding to the result of in vitro study, TPA treatment augmented the accumulation of RAW117-P cells in the liver. Fig. 5 shows the time-activity curve of the liver accumulation of these cells. TPA treatment augmented the

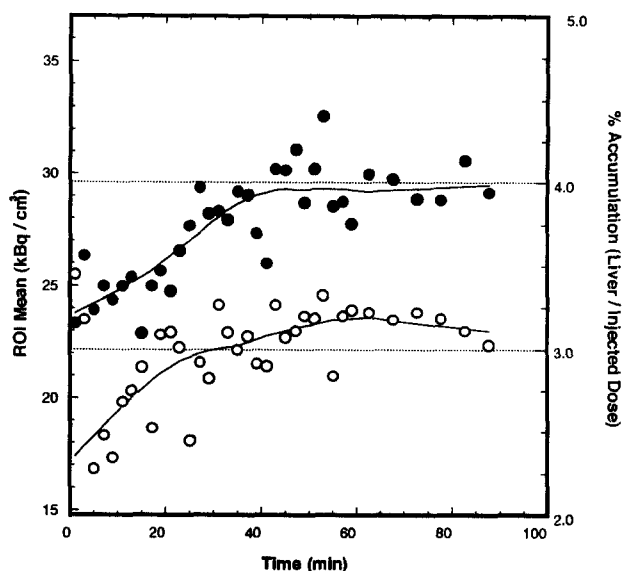


Fig. 5. Time-activity curves of ¹⁸F accumulation in the liver after injection of [2-¹⁸F]FDG-labeled RAW117-P cells treated or not with TPA. Time-activity curves of ¹⁸F in the liver after injection of [2-¹⁸F]FDG-labeled RAW117-P treated (●) or not (○) with TPA were obtained as described in Materials and methods.

accumulation of the cells in the liver from right after the injection to the end of the scanning period.

In contrast to the TPA treatment of the RAW117-P cells, Fig. 6 shows the suppression of the hepatic accumulation of RAW117-H10 by the treatment with H-7, an inhibitor of PKC. The suppression, however, occurred only right after injection of the cells. This is obvious by the time-activity curve shown in Fig. 7, where the suppression of the accumulation of H-7-treated cells was observed only during the first 30 min after injection of the cells. Such a phenomenon could not have been detected before the non-invasive method for analyzing real-time cell trafficking was developed. In this experiment, H-7-treatment did not affect FDG uptake or viability at least until the termination of the PET scanning.

4. Discussion

Metastasis occurs via a series of sequential steps [16,17]. Especially, in the organ-specific metastases, tumor cell adhesion to the venular endothelium of the target organ is thought to serve as an essential step after the detachment from the primary tumor sites and dissemination through the circulatory system [18]. Recent studies have indicated that the adhesion molecules of both tumor cells and endothelial cells of target organs play an important role in organ-specific metastases [19–24].

Positron emission tomography (PET) using [2-¹⁸F]FDG has been applied to cancer diagnosis, based on the higher metabolic demand of tumor cells than of non malignant cells this positron-labeled compound [25–27]. In the pre-

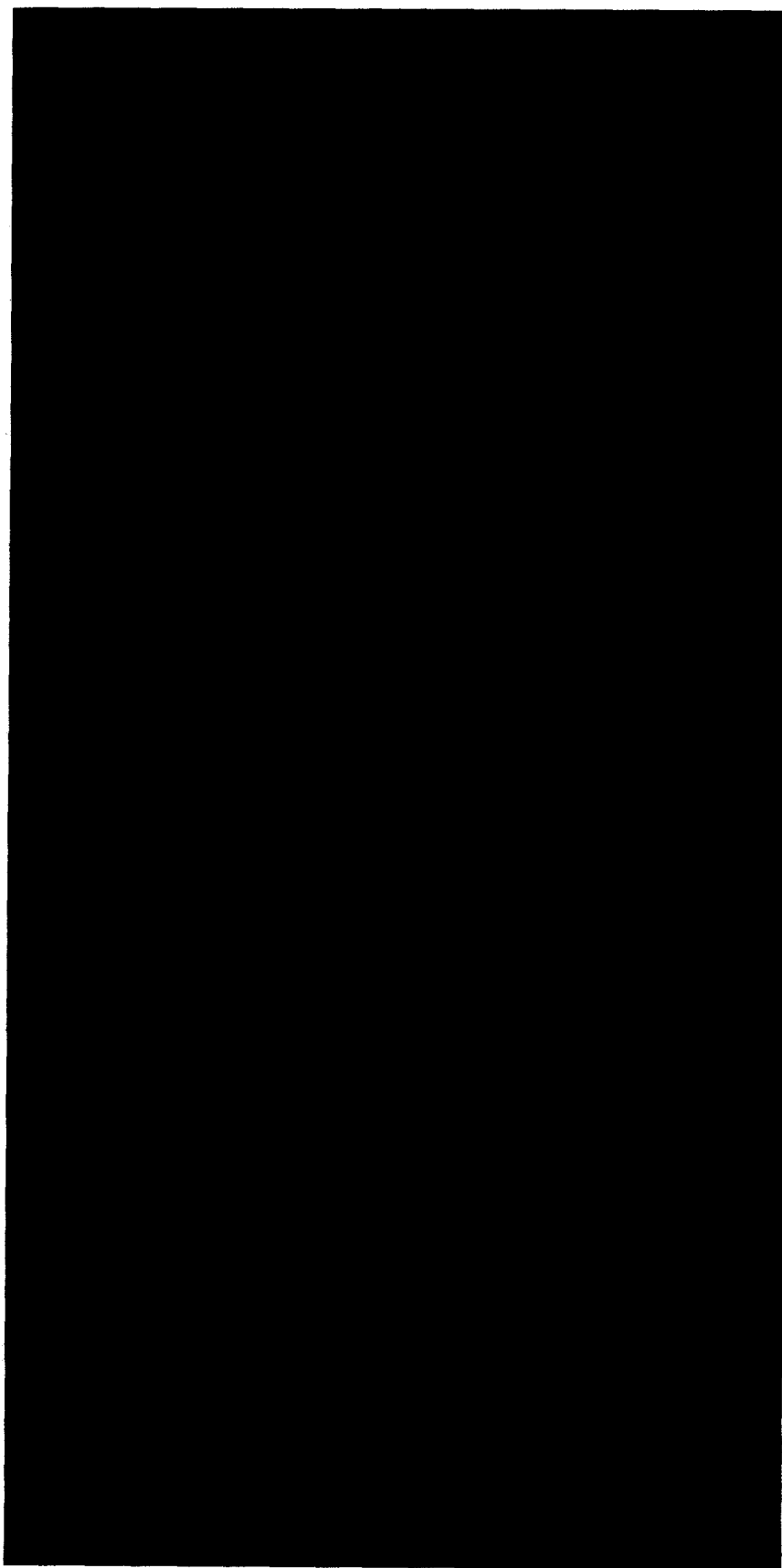


Fig. 6. Effect of H-7 on RAW117-H10 cell accumulation in the liver. Liver accumulation of [18 F]FDG-labeled RAW117-H10 treated or not with H-7 was determined by PET as described in Materials and methods. Status of the accumulation of the cells during the first 30 min after injection of the cells, during the next 30 min, and during the 60-to-90 min period post injection is shown.

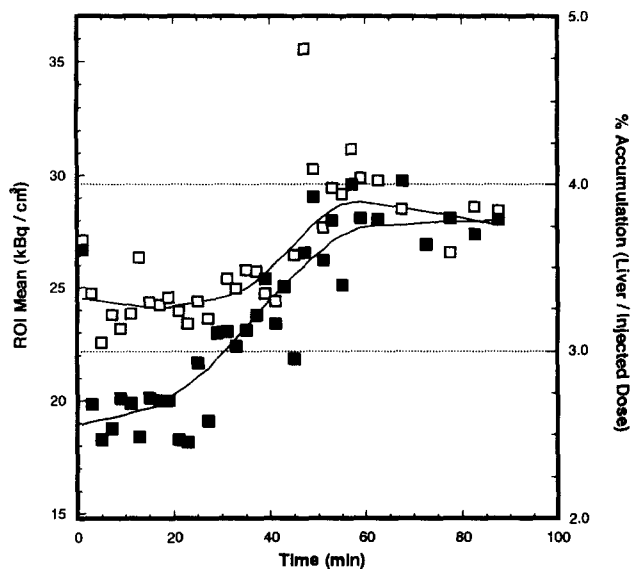


Fig. 7. Time-activity curves of ^{18}F accumulation in the liver after injection of $[2\text{-}^{18}\text{F}]\text{FDG}$ -labeled RAW117-H10 cells treated or not with H-7. Time-activity curves of ^{18}F in the liver after injection of $[2\text{-}^{18}\text{F}]\text{FDG}$ -labeled RAW117-H10 treated (■) or not (□) with H-7 were obtained as described in Materials and methods.

sent study, we used FDG as a simple labeling agent of metastatic tumor cells. Thus PET could detect real-time cell trafficking in vivo. When we examined the trafficking of RAW117 large cell lymphomas with different metastatic potential, i.e., parental RAW117-P and the highly liver metastatic subline RAW117-H10, we observed that the subline cells tended to accumulate more in the liver than the parental, although the accumulation of both types of cell in the lungs was more intense than that in the liver due to the passage of the cells through this organ first after i.v. injection.

Previous observations suggested that the reason for the higher metastatic potential of RAW117-H10 for the liver than that of parental RAW117-P is due to (1) the higher adhesiveness of RAW117-H10 to hepatic sinusoidal microvessel endothelium (HSE) [28], (2) deletion of membrane markers important for macrophage-mediated cytostasis [29], or (3) the softness of RAW117-H10 cell membrane which may cause the higher deformability in narrow vessels [30]. Against the first reason, a study involving the determination of cells accumulated in removed organs showed no correlation between accumulation of cells in vivo and metastatic potential [31]. On the contrary, the non-invasive PET study presented here indicated that the actual accumulation of metastatic cells in the target organ could be correlated with the metastatic potential and with the adhesiveness in vitro toward HSE. This discrepancy occurred because our experimental system can detect the rather weaker adhesion in vivo that can not be detected by invasive methods such as removal of organs.

Furthermore, the correlation between adhesion properties and in vivo trafficking was confirmed by the modulation of PKC, which affected adhesion of RAW117 cells.

Thus, PKC activation by TPA treatment of RAW117-P cells increased the degree of adhesion of the cells to HSE in vitro. Also, a greater accumulation of these cells in the liver was seen in vivo. On the contrary, PKC inactivation of RAW117-H10 by H-7 suppressed both in vitro adhesion and in vivo accumulation of the cells in the liver. The suppression of H-7-treated RAW117-H10 accumulation in liver was observed only during the first 30 min after administration of the cells. The reason that suppression did not last for long time is not clear at present. One possibility is that the adhesion molecules which are not regulated by PKC activity play a role at the later stage of PET scanning.

Although the correlation between metastatic behavior and adhesiveness of tumor cells is not fully understood, and although several different determinants on cell surfaces may be involved in these processes, our data clearly indicate that the adhesiveness of RAW117 cells to HSE in vitro is critical for the trafficking of these cells in vivo.

Several previous reports have indicated an effect of PKC modulation on metastasis: the adhesion rate of tumor cells to capillary endothelial cells is reported to be enhanced by phorbol esters through enhancement of their binding capacity without affecting their affinity for the endothelium [32]. Conformational changes of adhesion molecules induced by the phosphorylation may affect their binding characteristics for their ligands [33]. Especially, integrins, which may play an important role in the binding of the metastatic tumor cell to endothelium, have been shown to be substrates for PKC [34,35]. PKC is also reported to be involved in signal transduction of TNF in a number of types of tumor cells including lymphoid cell lines, where TNF caused a transient activation and translocation of PKC [36]. A number of studies demonstrated that PKC plays a critical role in metastatic cell behavior [4,9,11]. The present study clearly demonstrates that the modulation of PKC influenced the in vivo trafficking of metastatic tumor cells. The trafficking of tumor cells may be affected by other factors that are not assessable in simple in vitro adhesion assay systems. For example, LPS, IL-1 β and IFN- γ are potent inducers of cell adhesion. These molecules enhance cell binding by altering the endothelial cell-adhesive properties without having direct effects on tumor cells [37–39].

In conclusion, the adhesion properties of metastatic cells may be of critical importance for in vivo accumulation of the cells in the target organ, although the differential accumulation of cells of high and low metastatic potential could be detected only by the non-invasive method since a subtle difference in initial binding of metastatic cells to the endothelium may not be determined due to the bulk dissociation of weakly bound cells during the determination by the invasive method. The PET technique presented here may also clarify the determinant surface molecules through monitoring of overall in vivo trafficking of tumor cells.

Acknowledgements

The authors thank Ms. Ayano Takiguchi, Mr. Shingo Nishiyama, and Mr. Tsuyoshi Kosugi for their technical assistance.

References

- [1] Oku, N., Koike, C., Sugawara, M., Tsukada, H., Irimura, T. and Okada, S. (1994) *Cancer Res.* 54, 2573–2576.
- [2] Brunson, K.W. and Nicolson, G.L. (1978) *J. Natl. Cancer Inst.* 61, 1499–1503.
- [3] Kolber, M.A., Quinones, R.R., Gress, R.E. and Henkart, P.A. (1988) *J. Immunol. Methods* 108, 255–264.
- [4] Gopalakrishna, R. and Barsky, S.H. (1988) *Proc. Natl. Acad. Sci. USA* 85, 612–616.
- [5] Cavender, D.E., Edelbaum, D. and Welkovich, L. (1991) *J. Leukoc. Biol.* 49, 566–578.
- [6] Bereta, J., Bereta, M., Cohen, S. and Cohen, M. (1991) *J. Cell Biochem.* 47, 62–78.
- [7] Herbert, J.M. and Maffrand, J.P. (1991) *J. Cell Biochem.* 14, F407.
- [8] Herbert, J.M. and Maffrand, J.P. (1991) *Biochem. Pharmacol.* 42, 163–170.
- [9] Takenaga, K. and Takahashi, K. (1986) *Cancer Res.* 46, 375–380.
- [10] Brown, P.J. (1988) *Biochim. Biophys. Res. Commun.* 155, 603–607.
- [11] Dumont, J.A., Jones, W.D. and Bitonti, A.J. (1992) *Cancer Res.* 52, 1195–1200.
- [12] Freed, E., Gailit, J., Van der Geer, P., Ruoslahti, E. and Hunter, T. (1989) *EMBO J.* 8, 2955–2965.
- [13] Parise, L.V., Criss, A.B., Nannizzi, L. and Wardell, M.R. (1990) *Blood* 75, 2363–2368.
- [14] Hirst, R., Howitz, A., Buck, C. and Rohrscheider, L. (1986) *Proc. Natl. Acad. Sci. USA* 83, 6470–6474.
- [15] Nicolson, G.L., Belloni, P.N., Tressler, R.J., Dulski, K., Inoue, T. and Cavanaugh, P.G. (1989) *Invasion Metastasis* 9, 102–116.
- [16] Nicolson, G.L. (1988) *Cancer Metastasis Rev.* 7, 143–188.
- [17] Pauli, B.U., Augustin-Voss, H.G., El Sabbah, M.E., Johnson, R.C. and Hammer, D.A. (1990) *Cancer Metastasis Rev.* 9, 175–189.
- [18] Belloni, P.N. and Tressler, R.J. (1990) *Cancer Metastasis Rev.* 8, 353–389.
- [19] Natali, P., Nicotra, M.R., Cavaliere, R., Bigotti, A., Romano, G., Temponi, M. and Ferrone, S. (1990) *Cancer Res.* 50, 1271–1278.
- [20] Johnson, J.P., Stade, B.G., Holzmann, B., Schwable, W. and Riethmuller, G. (1989) *Proc. Natl. Acad. Sci. USA* 86, 641–644.
- [21] Chen, F.A., Repasky, E.A. and Bankert, R.B. (1991) *J. Exp. Med.* 173, 1111–1119.
- [22] Roosien, F.F., De Kuiper, P.E., De Rijk, D. and Roos, E. (1990) *Cancer Res.* 50, 3509–3513.
- [23] Rice, G.E. and Bevilacqua, M.P. (1989) *Science* 246, 1303–1306.
- [24] Quackenbush, E.J., Vera, S., Greaves, A. and Latarte, M. (1990) *Mol. Immunol.* 27, 947–955.
- [25] Haberkorn, U., Strauss, L.G., Dimitrakopoulou, A., Seiffert, E., Oberdorfer, F., Ziegler, S., Reisser, C., Doll, J., Helus, F. and Van Kaick, G. (1993) *J. Nucl. Med.* 34, 12–17.
- [26] Sasaki, M., Ichiyama, Y., Kuwabara, Y., Otsuka, M., Fukumura, T., Kawai, Y., Koga, H. and Masuda, K. (1993) *J. Nucl. Med.* 34, 288–290.
- [27] Hoffman, J.M., Waskin, H.A., Schifter, T., Hanson, M.W., Gray, L., Rosenfeld, S. and Coleman, R.E. (1993) *J. Nucl. Med.* 34, 567–575.
- [28] Nicolson, G.L. (1988) *Biochim. Biophys. Acta* 948, 175–224.
- [29] Yoshida, M., Gallick, G.E., Irimura, T. and Nicolson, G.L. (1987) *Cancer Res.* 47, 2558–2562.
- [30] Makino, K., Taki, T., Ogura, M., Handa, S., Nakajima, M., Kondo, T. and Ohshima, H. (1993) *Biophys. Chem.* 47, 261–265.
- [31] Reading, C.L., Kraemer, P.M., Miner, K.M. and Nicolson, G.L. (1983) *Clin. Expl. Metastasis* 1, 135–131.
- [32] Herbert, J.M. (1993) *Biochem. Pharmacol.* 45, 527–537.
- [33] Sibley, D.R., Berovic, J.L., Caron, M.G. and Lefkowitz, R.J. (1987) *Cell* 48, 913–922.
- [34] Hirst, R., Howitz, A., Buck, C. and Rohrscheider, L. (1986) *Proc. Natl. Acad. Sci. USA* 83, 6470–6474.
- [35] Van Leeuwen, R.L., Dekker, S.K., Arbiser, J.L., Vermeer, B.J., Bruijn, J.A., Byers, H.R. (1994) *Int. J. Cancer* 57, 894–900.
- [36] Schutze, S., Notrott, S., Pfizenmaler, K. and Kronke, M. (1990) *J. Immunol.* 144, 2604–2608.
- [37] Yu, C.L., Haskard, D.O., Cavender, D., Johnson, A.R. and Ziff, M. (1985) *Clin. Exp. Immunol.* 62, 554–560.
- [38] Cavender, D., Haskard, D.O., Joseph, B. and Ziff, M. (1986) *J. Immunol.* 136, 203–207.
- [39] Yu, C.L., Haskard, D.O., Cavender, D. and Ziff, M. (1986) *J. Immunol.* 136, 569–573.